J Electr Eng Technol.2018; 13(1): 201-210
http://doi.org/10.5370/JEET.2018.13.1.201

ISSN(Print) 1975-0102
ISSN(Online) 2093-7423

A New Start-up Method for a Load Commutated Inverter for Large Synchronous Generator of Gas-Turbine

Hyunsung An* and Hanju Cha†

Abstract – This paper proposes a new start-up method for a load commutated inverter (LCI) in a large synchronous gas-turbine generator. The initial rotor position for start-up torque is detected by the proposed initial angle detector, which consists of an integrator and a phase-locked loop. The initial rotor position is accurately detected within 150ms, and the angle difference between the real position and the detected position is less than 1%. The LCI system operates in two modes (forced commutation mode and natural commutation mode) according to operating speed range. The proposed controllers include a forced commutation controller for the low-speed range, a PI speed controller and a PI current controller, where the forced commutation controller is connected to the current controller in parallel. The current controller is modeled by Matlab/Simulink, where a six-pulse delay of the thyristor and a processing delay are considered by using a zero-order hold. The performance of the proposed start-up method is evaluated in Matlab/Psim at standstill and at low speed. To verify the feasibility of the method, a 5kVA LCI system prototype is implemented, and the proposed initial angle detector and the system performance are confirmed by experimental results from standstill to 900rpm.

Keywords: Gas-turbine, Static frequency converter, Load commutated inverter, Start-up method, Initial rotor position detection

1. Introduction

A gas-turbine generator system needs a start-up system for internal combustion, and the fuel of the gas-turbine system begins to combust at approximately 30% of the rated speed [1]. Before the 1990s, start-up systems used a DC motor or an induction machines. In case the conventional methods, the DC motors had maintenance problems, and the induction machines had shaft vibration problems. Due to these problems, static frequency converter (SFC) systems using semiconductor switches have been studied as a start-up system of gas turbines since the 1990s [2-5]. An SFC system is used in variable applications like pumped storage systems, gas-turbine and start-up systems for large-scale synchronous machines [6-10]. The SFC system can be applied to multiple gas-turbine system through one device. The gas turbines range from several megawatts up to several hundred megawatts, and the SFC systems range from several hundred kilowatts up to several megawatts.

The SFC system is applied to a current source inverter (CSI) because it is a large-scale system, and one generally used SFC system is a load commutated inverter (LCI) [11-14]. The switching devices in an LCI system are a thyristors, rather than insulated gate bipolar transistors (IGBTs). Although thyristor switches have the uncontrollable characteristics of turn-off, the thyristors can guarantee the reliability than other switching devices when applied to high voltages and high current in a large-scale power station system. Generally, current in the switch must be reduced to zero, or the voltage across the switch must be reversed in order to turn off a thyristor. However, with a motor drive system that operates in variable voltages and frequency, a different operating method must be applied at the LCI system because of the insufficient induced voltage of the synchronous machine in the initial start-up. So, the LCI system for switch turn-off operates in two modes, which are forced (or pulse) commutation mode at low-speed ranges and natural commutation mode at middle- and high-speed ranges [15, 16].

It is important to know the rotor position of a synchronous machine in order to obtain the start-up torque for initial start-up with respect to operation in forced commutation mode. The thyristor pair at the stopped state of the synchronous machine is determined according to the initial rotor position, and the LCI system need the absolute rotor position of the synchronous machine. Detection methods for the initial rotor position by using thyristor converter are limited due to the turn-off characteristic of the thyristor switch, although there are many methods that detect the initial rotor position for IGBT based power conversion system [17-19]. When encoder are used, the variation rate of the rotor position can be detected, but the absolute initial rotor position cannot be known before generating a z-pulse despite using an encoder-based system. Therefore, a synchronous machine is operated by arranging

† Corresponding Author: Dept. of Electrical and Electronic Engineering, Chungnam National University, Korea. (hjcha@cnu.ac.kr)
* Dept. of Electrical and Electronic Engineering, Chungnam National University, Korea.(hsan@cnu.ac.kr)
Received: February 8, 2017; Accepted: August 24, 2017

the rotor in a specific position or by distinguishing the polarity of the terminal voltage via injection of field current [20]. Back-electromotive force (back-emf) in the synchronous machine is temporarily induced at the moment of field current injection, and the magnitude and polarity of the induced back-emf vary according to rotor position. Polarity of the back-emf is separated into six sectors and a pair of thyristors fire in accordance with polarity. It is difficult to know the exact rotor position, although the approximate rotor position is known. The distinguished polarity can incorrectly determine the rotor position because of noise in the zero-crossing area. Incorrect information as to rotor position causes erroneous thyristor selection, which then cannot create the proper start-up torque.

This paper proposes a detection method of the initial rotor position by using an integrator and a phase-locked loop (PLL) simply for a stable start-up method of a synchronous machine. Modeling of the current controller was designed in Simulink/Matlab for stable operation in forced commutation mode. The performance of the proposed initial angle detector and the performance of the LCI system were verified through simulation and experimental results.

2. Gas-Turbine and Start-up System

Fig. 1 shows the overall system of a gas-turbine power station that consists of a gas-turbine, a synchronous generator, an LCI system, an excitation system and other systems of a power station. A gas-turbine generator system needs an LCI system for initial start-up of the gas-turbine. The large synchronous machine of power station operates as a motor before the grid connection. When the rated speed is reached, the synchronous machine operates as a generator. A governor for generator, LCI and excitation system are operated by a main control system according to command of control room in the power station. Fig. 2 shows the structure of the conventional method through an induction machine, which includes an additional coupling shaft and machine. This method is not appropriate because

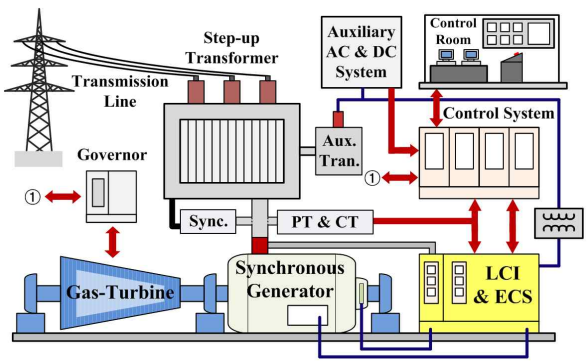

Fig. 1. Configuration of a gas-turbine power station

of the maintenance problem and shaft vibration. Therefore, a start-up system is applied to an LCI system. Fig. 3 shows the operating characteristic curve of a gas turbine and an LCI system. A gas turbine is generally driven by grid frequency, and an LCI system operates until 90% of the gas-turbine grid frequency.

2.1 Load commutated inverter

Fig. 4 shows the structure of an LCI system, which consists of a supply-side thyristor converter, a machine-side thyristor converter, a synchronous machine, an exciter and a controller for stable operation of the system. The

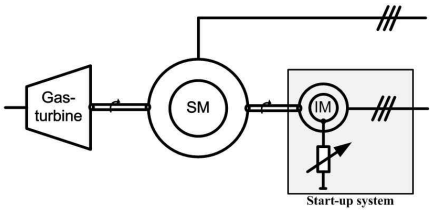

Fig. 2. Conventional method for a start-up system

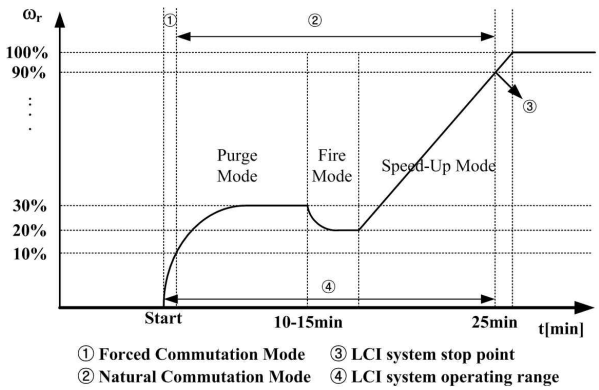

Fig. 3. Operating characteristic curve of a gas-turbine system

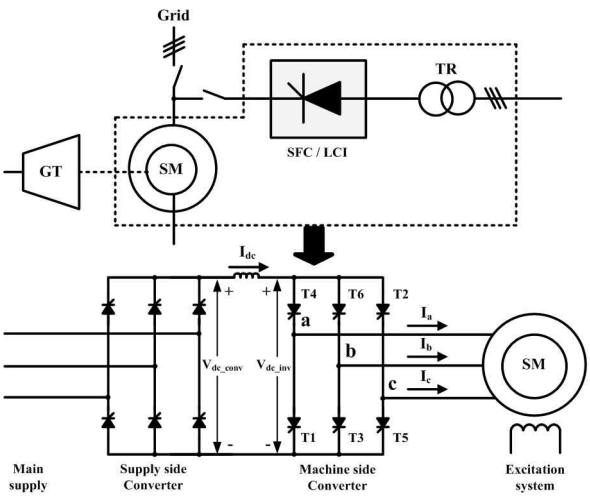

Fig. 4. Configuration of an LCI system

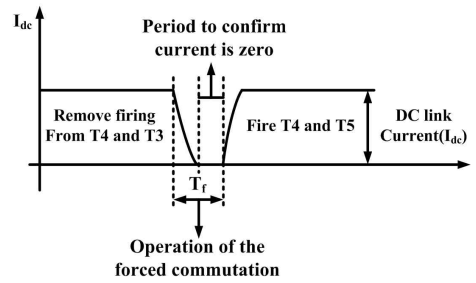

Fig. 5. Principle of forced commutation mode

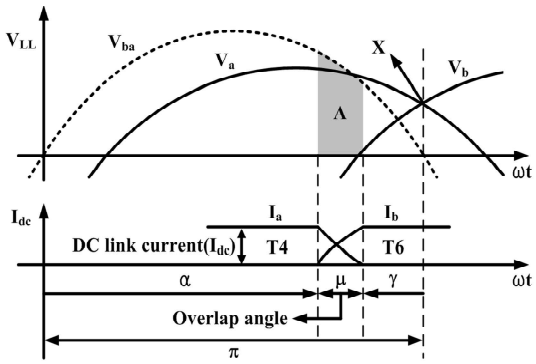

Fig. 6. Principle of natural commutation mode

load commutated inverter employs a DC reactor between the supply-side thyristor converter and the machine-side thyristor converter. The supply-side converter is a thyristor based three phase six-pulse bridge circuit in which constant three-phase AC voltage is converted into variable DC voltage. The machine-side converter is also a thyristor based three-phase six-pulse bridge circuit in which the DC voltage generated by the supply-side converter is inversely converted to three-phase AC power with a variable amplitude and a variable frequency.

2.2 Commutation modes

The load commutated inverter system operates in two modes: forced (or pulse) commutation mode and natural commutation mode. The operation modes of the LCI system are classified by the turn-off characteristics of the thyristor. At low speed, the level of the induced back-emf is too low to ensure correct switching of the converter thyristors. So, forced commutation mode is used for initial starting or at low speed in the machine. This forced commutation sequence is shown in Fig. 5, where the rates of reduction and the increase in current are dictated by the circuit voltage levels and the value of the DC link reactor.

When the machine is generating sufficient voltage at its terminals to allow satisfactory natural commutation of the machine converter thyristors, the drive operates in normal running mode. This is shown in Fig. 6, which shows the waveforms occurring during the process of switching from thyristors 4 to 6. When the T6 is turn on, because V_a is more than V_b, cause the current in thyristor 4 to reduce and

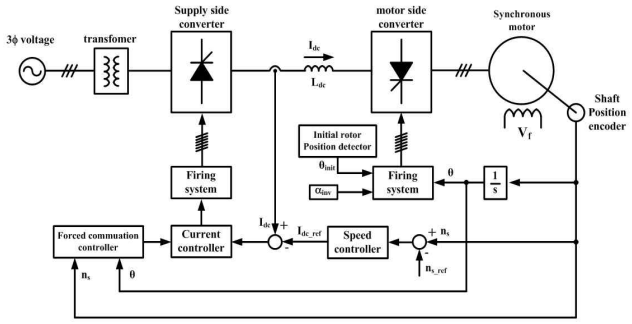

Fig. 7. Control structure of an LCI system

that in thyristor 6 to increase. The rate of change of these currents depends on the value of the effective inductance of the machine and the magnitude of the voltages while the current is changing. In addition the period when both thyristors are conducting (the overlap angle) will depend on the level of current flowing in the circuit. The overlap period must be completed before point X is reached otherwise the voltage which is causing the current transfer will reverse and the transfer will not be completed, resulting in an inversion failure and a high fault current in the circuit.

3. Control Methods of an LCI system

Fig. 7 shows the control structure of an LCI system that consists of a PI speed controller for purge mode of the gas turbine, a PI current controller, and a forced commutation controller. Additionally, the LCI system added an initial rotor position detector to determine the thyristor pair for large torque. The stator current vector in the synchronous machine is injected so as to be vertical with respect to rotor flux for large-torque generation. Rotor position information is obtained by a position sensor, and the machine-side converter operates through constant firing angles. The supply-side converter operates through variable firing angles via calculations of the current controller and the forced commutation controller.

3.1 Detection of initial rotor position

It is important to select a pair of thyristors according to rotor position in order to inject large torque at initial start-up. The initial rotor position cannot be known before generating an initial z-pulse, despite using an encoder-based system. Field current is used to detect the initial rotor position and the back-emf is induced in the stator of the synchronous machine after injecting field current. The induced back-emf has various magnitudes and polarity, depending on rotor position. Induced back-emf is expressed in (1), (2) and (3). α_a, α_b, and α_c show the difference of angles between each terminal axis and the rotor position, as shown Fig. 8. X references the rotor

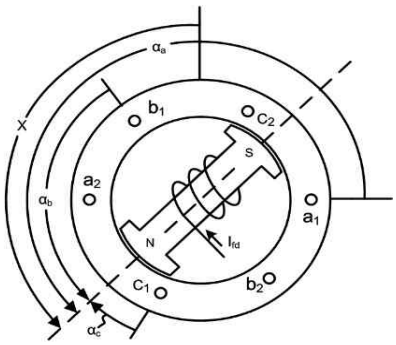

Fig. 8. Simplified representation of a silent-pole synchronous machine

Table 1. Relationship between rotor position and polarity of back-emf

Rotor position	Polarity Combination		
	E_a	E_b	E_c
0°~60°	-	+	-
60°~120°	-	+	+
120°~180°	-	-	+
180°~240°	+	-	-
240°~300°	+	-	+
300°~0°	+	+	-

position, and i_{fd} and k are field current and slope of the field current. The relations to polarity can be represented in six sectors, as shown Table 1, and thyristor pairs are selected by these polarities. However, this method can give rise to a problem at initial start-up due to mistaken selection of the thyristor pair from a wrong decision about polarity at the zero-crossing point in back-emf.

$$E_a = k\frac{di_{fd}}{dt}\cos\alpha_a \tag{1}$$

$$E_b = k\frac{di_{fd}}{dt}\cos\alpha_b \tag{2}$$

$$E_c = k\frac{di_{fd}}{dt}\cos\alpha_c \tag{3}$$

The proposed method uses the relationship between back-emf and rotor flux of the synchronous machine. Since back-emf and rotor flux have a phase difference of 90 degrees, rotor flux can be estimated by using the induced back-emf at field current injection.

The terminal voltage (V_{ds}^s, V_{qs}^s) in a stationary reference frame is expressed in (4) and (5), where R_s, L_{dq}, i_{dqs}^s and e_{dqs}^s represent stator resistance, d-q axis inductance, stator current in the stationary reference frame and back-emf in the stationary reference frame, respectively.

$$V_{ds}^s = I_{ds}^s R_s + L_d\frac{d}{dt}i_{ds}^s + e_{ds}^s \tag{4}$$

$$V_{qs}^s = I_{qs}^s R_s + L_q\frac{d}{dt}i_{qs}^s + e_{qs}^s \tag{5}$$

The back-emf component by field flux is proportional to the delta value in field flux. So, back-emf is expressed in (6) and (7), where θ_{init}, λ_{dqr}^s and λ_f represent initial rotor position, d-q axis rotor flux and field flux, respectively.

$$e_{ds}^s = \frac{d}{dt}\left(\lambda_{dr}^s\right) = \frac{d}{dt}\left(\lambda_f\cos\theta_{init}\right) \tag{6}$$

$$e_{qs}^s = \frac{d}{dt}\left(\lambda_{qr}^s\right) = \frac{d}{dt}\left(\lambda_f\sin\theta_{init}\right) \tag{7}$$

In the build-up state for field current, stator current (i_{dqs}^s) is zero in (4) and (5). Therefore, terminal voltage of the machine is equal to back-emf, which is represented in (8) and (9).

$$\lambda_{dr}^s = \int V_{ds}^s dt = \int e_{ds}^s dt \tag{8}$$

$$\lambda_{qr}^s = \int V_{qs}^s dt = \int e_{qs}^s dt \tag{9}$$

Fig. 9 shows a block diagram of the method for detecting initial angle, which consists of the integrator and the PLL. The PLL can accurately estimate rotor position and speed without system parameters such as inertia and torque. The PLL for estimation of the initial rotor position is shown in Fig. 10, and input of PLL is the estimated rotor flux. The difference angle between estimated rotor position and real rotor position is compensated by proportional integral (PI) controller. It is easy to detect the absolute position of the rotor,and it does not cause a problem in DC drift of a pure integrator owing to detection of rotor position within 150ms. The detected initial rotor position is accurate to within 1% to the actual position via encoder, and thyristor pair determined through the exact initial rotor position shown in Table 2. In this paper, reference to rotor position is synchronized line-to-line in the A phase and C phase, and the firing angle of the machine-side converter is determined to be a constant value at 150 degrees.

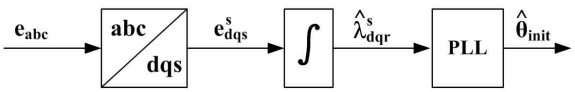

Fig. 9. Block diagram of initial angle detection

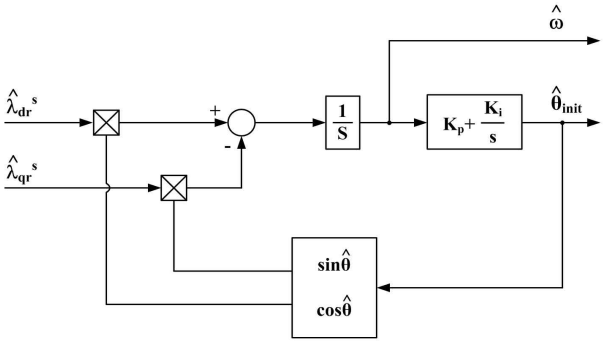

Fig. 10. Block diagram of PLL

Table 2. Relationship between rotor position and thyristor pair

Rotor position	Thyristor pair
330°~ 30°	T3, T4
30°~ 90°	T4, T5
90°~ 150°	T5, T6
150°~ 210°	T6, T1
210°~ 270°	T1, T2
270°~ 330°	T2, T3

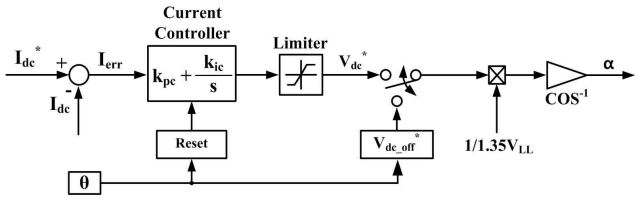

Fig. 11. Block diagram of the current controller

3.2 Current controller and forced commutation

Fig. 11 shows a block diagram of the current controller and the forced commutation controller connected to the current controller in parallel. The current controller generates the DC link voltage reference (V_{dc}^{*}) for the firing angle of the supply-side converter, and the forced commutation controller generates the voltage reference ($V_{dc\_off}^{*} = 150V$) for zero amperes (0A) in DC current. Firing angle can be calculated through the $\cos\theta^{-1}$ block of Fig. 11, and the DC voltage (V_{dc_conv}) on the supply side is expressed in (10). Firing angle of the supply-side converter is calculated through $\cos\theta^{-1}$, as seen in (11). V_{s_LL} and α_{conv} are the supply voltage and firing angle of the supply side. The current controller is reset to prevent saturation of the integrator during operation in forced commutation mode. The current controller is important for a stable start-up state in forced commutation mode, and performance of the current controller is required for the desired response time and accuracy, because the firing pulse for forced commutation is generated in order to turn off the thyristors on the machine side at intervals of 60 degrees, as shown in Fig. 12. So, performance of the controller must be confirmed by controller loop modeling of the thyristor converter through Matlab/Simulink. Modeling of the controller consists of the PI controller, the output limit of the controller, the thyristor six-pulse delay and the plant. Six-pulse delay is implemented by zero-order hold, and the plant is composed of DC reactance (140mH). The value of the zero-order hold is set to 2.78ms due to the six-pulse operation, and the sampling time of the digital processor is 200μs. The machine-side converter does not get considered because of the constant firing control. Current controller gains are designed to satisfy a phase margin of 67 degrees, and performance of the current controller was confirmed by overshoot, rising time and phase margin. Rising time and overshoot are 9.2ms and

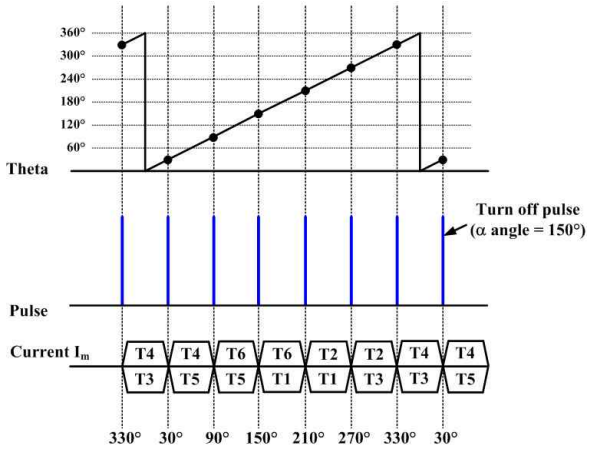

Fig. 12. Principle of forced commutation

380mA, and controller gain by modeling is applied in the real LCI system. Controller modeling was verified through comparison of simulation and experimental results in the section 4 and 5.

$$e_{ds}^{s} = \frac{d}{dt}\left(\lambda_{dr}^{s}\right) = \frac{d}{dt}\left(\lambda_{f}\cos\theta_{init}\right)$$
$$= 1.35V_{s\_LL}\cos\alpha_{conv} \quad (10)$$

$$\alpha_{conv} = \cos^{-1}\left(\frac{V_{dc\_conv}}{1.35\times V_{s\_LL}}\right) \quad (11)$$

4. Modeling and Simulation Results

Fig. 13 shows the modeling of the LCI system, which consists of supply/machine-side converters as three-phase six-pulse bridge connection circuits, a DC reactor, a synchronous machine, controller segments and the initial angle detection block. The simulation model was implemented through MATLAB, and the simulation was added through Psim in order to check precisely the performance such as the current controller, operation characteristic and so on. The simulation conditions are the same as the experimental conditions.

4.1 Detection of initial rotor position

Figs. 14 (a) and (b) show the performance of the initial angle detector according to the initial rotor position. The initial angle in Fig. 14 (a) is 50 degrees, and the initial angle in Fig. 14 (b) is 220 degrees. Initial rotor position was detected rapidly and accurately through the detector. The thyristor pair was determined by the initial angle, as shown in Table 2. The initial rotor position detector is no effect of the load because the LCI is operated by thyristor pair determined by the initial rotor position detector at the stopped state (zero speed) of the machine. In other words, initial rotor position detector operates before the switching

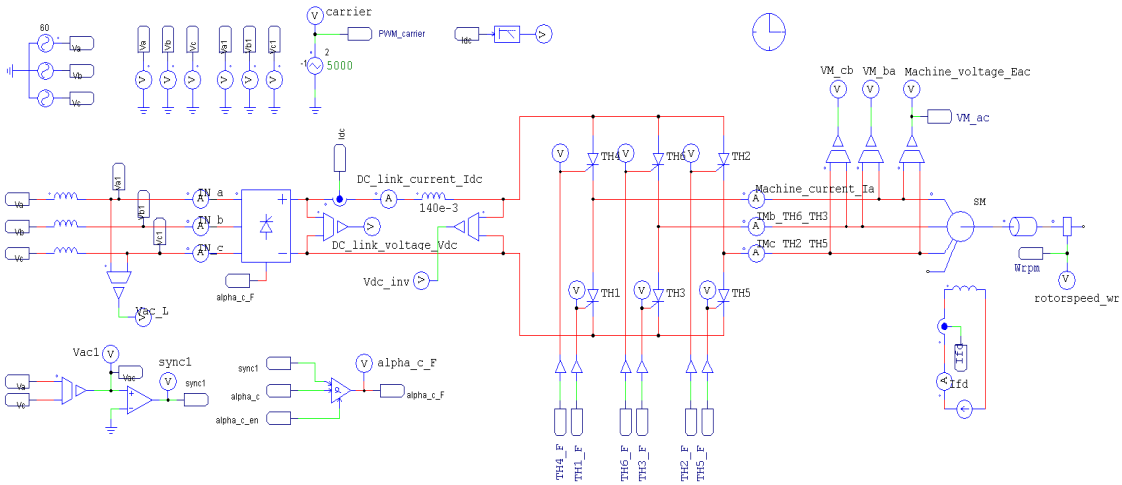

Fig. 13. Modeling of the load commutated inverter

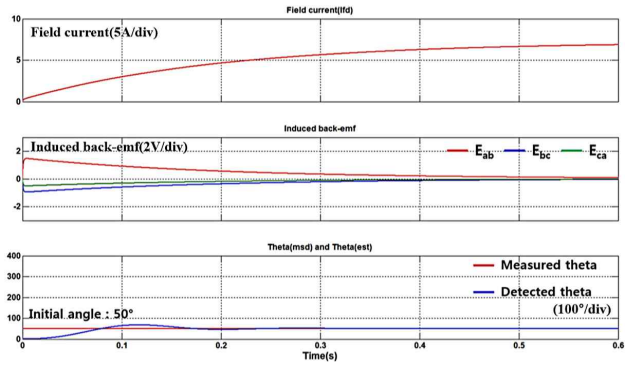

(a)

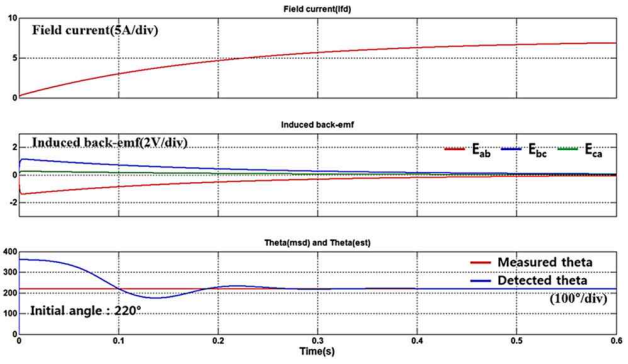

(b)

Fig. 14. Initial rotor position detection: (a) Initial angle : 50° (b) Initial angle : 220°

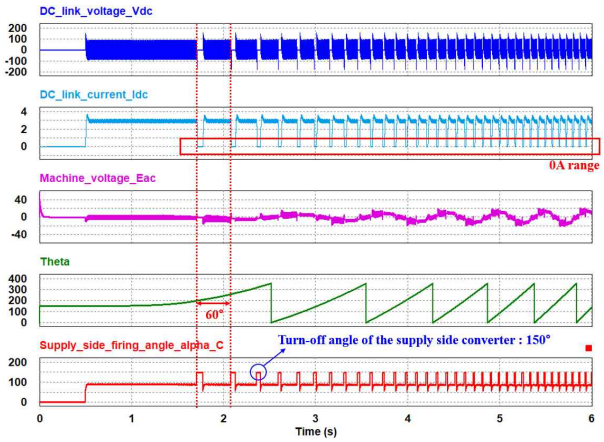

Fig. 15. Start-up within forced commutation mode

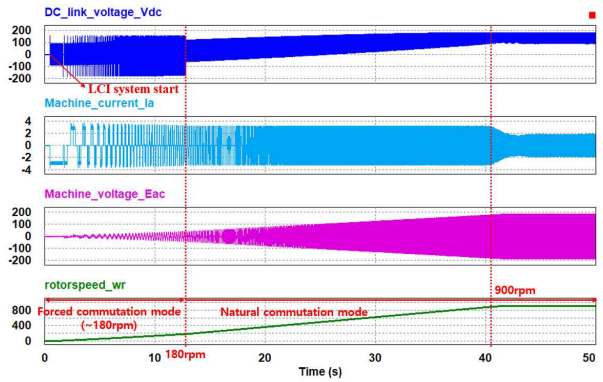

Fig. 16. Overall start-up of the LCI system

operation of the thyristor.

4.2 Start-up of the LCI system

Fig. 15 shows the operation in forced commutation mode, and the machine-side firing angle was determined by considering start-up torque and leading factor. In this paper, firing angle (α_{inv}) of the machine-side converter is a constant value at 150 degrees, and the rotor position is synchronized in E_{ac} (line to line) of the synchronous machine. Fig. 15 shows forced commutation mode at 150rpm, and machine input current is reduced to 0A from the level of the DC current for thyristor turn-off at 60 degrees. Additionally, the firing angle is changed by a forced current mode controller to 150 degrees as shown in the Fig. 15. The LCI system was confirmed to be in a

stable start-up state. Fig. 16 shows the overall start-up of the synchronous generator, and the speed command value was set at 900rpm in consideration of weak field range. Operation modes and speed/current control are sequential in accordance with the speed range. These simulation results show the performance of the LCI system.

5. Experimental Results

To verify the feasibility of the proposed methods, a 5kVA prototype was built. Fig. 17 shows the prototype 5kVA LCI system and a 5kVA motor-generator set (MG-set), with the power line as explained in the LCI system configuration in Section 2. DC reactance is 140mH. In addition, the LCI system is composed of an overall system controller (MCP), voltage/current sensors (PT/CT), a firing system (GPD) and DSP controller, and a field-programmable gate array (MGI) for desirable control of the LCI system. Synchronous machine parameters are show in Table 3. The performance of the LCI system was verified through initial angle detection and start-up of the LCI system in forced commutation mode.

Table 3. Parameters of the synchronous machine

Rated power	5kVA	d-axis inductance	22.6mH
Rated voltage	3Φ220V	q-axis inductance	11.3mH
Field current (no load)	4.9A	Field current (rated load)	8.1A
Field voltage (no load)	12.6V	Field voltage (rated load)	24.3V
Rated speed	1800rpm	Pole pair	2

Fig. 17. Prototype of the 5kVA LCI system and MG-set

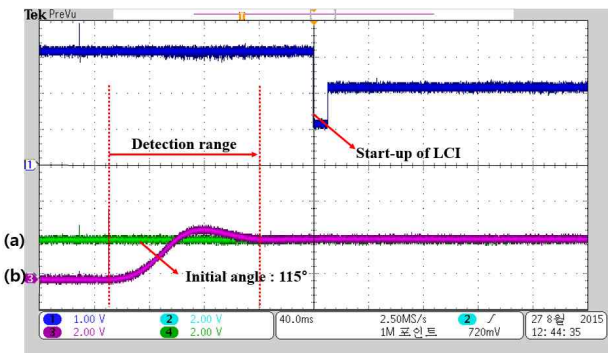

Fig. 18. Initial angle detection (θ_{init} = 115°): (a) Measured theta (2rad/div), (b) Detected theta (2rad/div)

5.1 Detection of initial rotor position

Fig. 18 and Fig. 19 show experimental results from initial angle detection according to initial rotor positions, which were 115 degrees and 230 degrees. Rotor position was detected rapidly and accurately within 150ms by the initial angle detector, and the angle error in detected position compared to the real position by the encoder was less than 1%. The LCI system can be operated with selection of the thyristor pair from initial rotor position information. Fig. 20 shows the relationship between initial angle detection and thyristor pair. The initial angle in Fig. 20 is 160 degrees, and the LCI system begins with thyristors 6 and 1; the switching relationship according to rotor position is shown in Table 2.

5.2 Start-up of the LCI system

Figs. 21 (a) and (b) show the step response of the DC

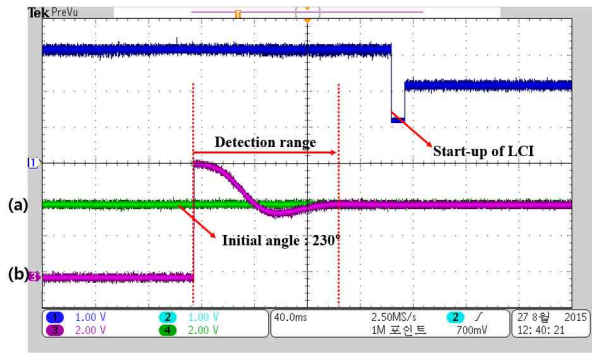

Fig. 19. Initial angle detection (θ_{init} = 230°): (a) Measured theta (2rad/div), (b) Detected theta (2rad/div)

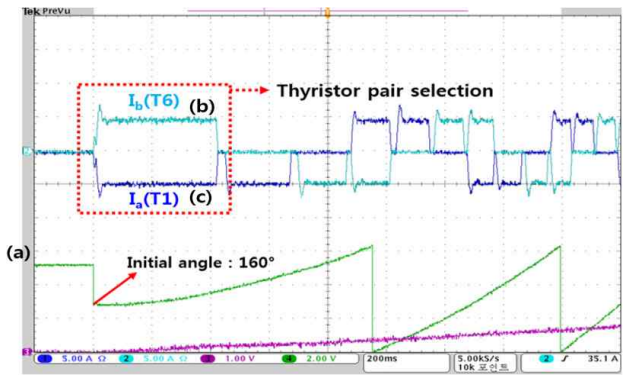

Fig. 20. Selection of thyristor pair: (a) Theta (θ, 2rad/div), (b) B phase input current, (c) C phase input current

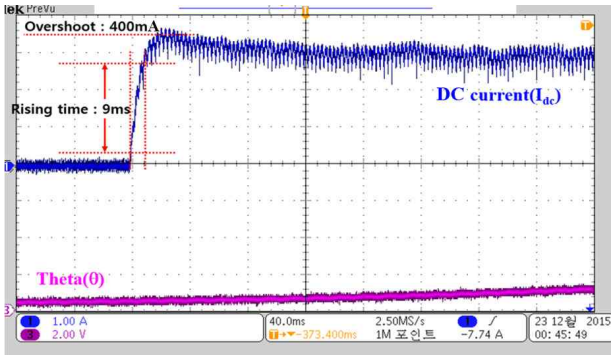

(a)

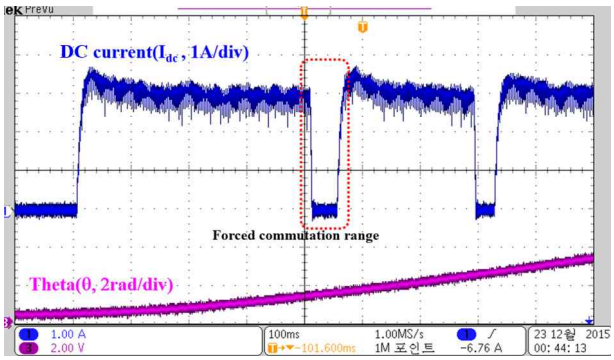

(b)

Fig. 21. Response of current control: (a) Step response of DC current, (b) DC link current from forced commutation

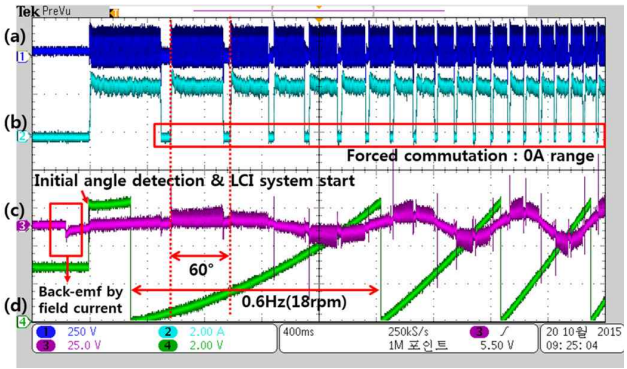

Fig. 22. Initial start-up in forced commutation mode: (a) DC link voltage (V_{dc}, 250V/div), (b) DC link current (I_{dc}, 2A/div), (c) machine voltage (E_{ac}, 25V/div), (d) Theta (θ, 2rad/div)

current and the DC current waveform in forced commutation mode, where DC current reference is a step value to 3A from 0A. Rising time and overshoot of DC current are 9ms and 400mA, as shown Fig. 21(a). These experimental results are well matched to results according to the modeling in Matlab, and confirmed that the current controller is designed well. Fig. 22 shows forced commutation mode to 50rpm from standstill, and DC current was reduced to 0A from the DC current level for

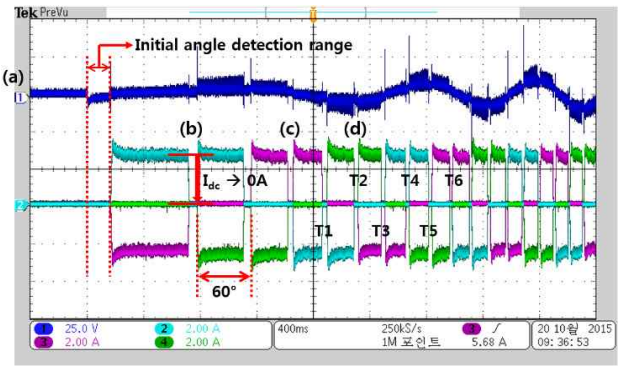

Fig. 23. Three-phase current in forced commutation mode: (a) Machine voltage (E_{ac}, 25V/div), (b) A-phase machine input current (I_a, 2A/div), (c) B-phase machine input current (I_b, 2A/div), (d) C-phase machine input current (I_c, 2A/div)

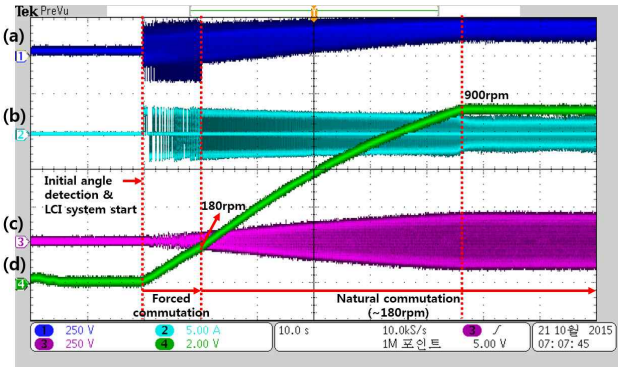

Fig. 24. Overall start-up of the LCI system: (a) DC link voltage (V_{dc}, 250V/div), (b) A-phase machine input current (I_a, 5A/div), (c) machine voltage (E_{ac}, 250V/div), (d) rotor speed (ω_r, 200rpm/div)

thyristor turn-off at 60 degrees. The DC link current reference is 3A, and supply-side voltage is three-phase 130V_{rms}. The DC link voltage of the supply-side converter is changed by firing angle ($\alpha_{inv} = 150°$) in forced commutation mode. Fig. 23 shows three-phase current (machine input current) in forced commutation mode. After initial angle detection, commutation performance in the low-speed range was confirmed through flow of the machine input current according to determination of the thyristor pair. Fig. 24 shows the overall start-up of initial angle detection, forced commutation and natural commutation. The speed reference was set at 900rpm in consideration of weak field range. Operation mode and speed/current control are sequential in accordance with the speed range. The LCI system was confirmed to be in a stable start-up state.

6. Conclusion

This paper proposed a start-up method for stable

operation of a large synchronous generator for gas-turbine, and the start-up system for the gas turbine applies a load commutation inverter in order to ensure stable start-up. Operation modes are applied forced commutation mode and natural commutation mode, considering thyristor turn-off characteristics. The initial angle detector consists of an integrator and a PLL, where initial rotor position is detected rapidly and accurately within 150ms through induced back-emf during initial field current build-up time. The detected rotor position matches position information from an encoder, with error less than 1%. The current controller of the LCI system has been designed by Matlab/ Simulink to verify PI current control. Six-pulse thyristor delay time and processing delay were considered using a zero-order hold, and current control of the LCI system was analyzed. The performance of the proposed start-up method and the current control were evaluated in Matlab/ Psim at standstill and at low speed. To verify the feasibility of the start-up method, a 5kVA LCI system prototype has been implemented, and the proposed initial angle detector and operation modes were confirmed by experimental results at overall speed range.

Acknowledgements

This work was supported by the Korea Electric Power Research Institute (KEPRI) grant funded by Korea Electric Power Corporation (KEPCO) (R16EA09)

References

[1] Seon-Hwan Hwang, Jang-Mok Kim, Ho-Seon Ryu and Gi-Gab Yoon, "Control Algorithm of Large Synchronous Machines for Starting Gas Turbosets," *Journal of Power Electronics*, vol. 9, no. 2, pp.146-155, Mar. 2009.

[2] Ryota Okuyama, Yasuaki Matsumoto, Hiroshi Ogino, Shigeyuki Nakabayashi, Akinobu Ando and Yasuhiko Hosokawa, "Compact Static Starting Device for Gas Turbine," *in Proceedings of IEEE ECCE Asia 2013*, June 2013

[3] S.D. Sudhoff, E.L. Zivi and T.D. Collins, "Start-up Performance of Load-Commutated Inverter Fed Synchronous Machine Drives," *IEEE Trans. Energy Conversion*, vol. 10, no. 2, pp. 268-274, Jun. 1995.

[4] Hisanori Taguchi, Shinzo Tamai, Yasuhiko Hosokawa and Akinobu Ando, "APS Control Method for Gas Turbine Start-up by SFC," *in Proceedings of IEEE IPEC 2010 International Conference*, Jun. 2010.

[5] Jin Guangzhe, Zhou Changcheng, Gao Qiang and Xu Dianguo, "Research on System of Self-controlled Soft Start with Variable Frequency for Synchronous Motor," *in Proceedings of IEEE IPEMC 2012 7th international conference,* Jun. 2012.

[6] Wang Keshun, Zhang Lichun, Yang Bo, Li Guanjun, Tao Yibin, Fu Jianzhong, Li Jianfeng and Ji Liantao, "Developing and Simulation Research of the Control Model and Control Strategy of Static Frequency Converter," *in Prprounoceedings of IEEE ISDEA 2012 Second International Conference*, Jan. 2012.

[7] Jung-Chen Chiang, Chi-Jui Wu and Shih-shong Yen, "Mitigation of Harmonic Disturbance at Pumped Storage Power Station with Static Frequency Con-vertet," *IEEE Trans. Energy Conversion*, vol. 12, no. 3, pp. 232-240, Sept. 1997.

[8] Chihiro Hasegawa and Shoji Nishikata, "A Simple Starting Method for Self-Controlled Synchronous Motors in Electric Propulsion Systems for Ships," *in Proceedings of IEEE Power Electronics and Applications, 2007 European Conference,* Sept. 2007.

[9] Arun Kumar Datta, M.A. Ansari, N. R. Mondal, B. V. Raghavaiah, Manisha Dubey and Shailendra Jain, "Simulation of Static Frequency Converter for Synchronous Machine Operation and Investigation of Shaft Voltage," *International Journal of Electrical, Computer, Energetic, Electronic and Communication Engineering*, vol. 8, no. 3, 2014.

[10] Greg Magsaysay, Thomas Schuette and Russ J. Fostiak, "Use of a Static Frequency Converter for Rapid Load Response in Pumped-Storage Plants," *IEEE Trans. Energy Conversion*, vol. 10, no. 4, pp. 1771-1782, Dec. 1995.

[11] kamalesh Hatua and V.T. Ranganathan, "A Novel VSI- and CSI-Fed Active-Reactive Induction Motor Drive with Sinusoidal Voltage and Currents," *IEEE Trans. Power Electronics*, vol. 26, no. 12, pp. 3936-3947, Dec. 2011.

[12] Eduardo P. Wiechmann and Rolando Burgos, "On the Efficiency of Voltage Source and Current Source Inverters for High-Power Drives," *IEEE Trans. Industrial Electronics*, vol. 55, no. 4, pp. 1771-1782, Dec. 2011.

[13] Amit Kumar Jain and V.T. Ranganathan, "Improved Control of Load Commutated Inverter Fed Salient Pole Wound Field Synchronous Motor Using Field Oriented Technique," *in Proceedings of IEEE ECCE 2012 Conference*, Sept. 2012.

[14] Bhim Singh, Sanjeev Singh and S.P. Hemanth Chender, "Harmonics Mitigation in LCI-Fed Synchronous Motor Drives," *IEEE Trans. Energy Conversion*, vol. 25, no. 2, pp. 369-380, June 2010.

[15] David Finney, "Variable frequency AC motor drive systems," Peter Peregrinus Ltd, 1988, pp. 202-274.

[16] Alberto Tessarolo and Roberto Menis, "On the Modeling of Commutation Transients in Split-Phase Synchronous Motors Supplied by Multiple Load-Commutated Inverters," *IEEE Trans. Industrial Electronics*, vol. 57, no. 1, pp. 35-43, Jan. 2010.

[17] Chihiro Hasegawa and Shoji Nishikata, "A Sensorless Rotor Position Detecting Method," *in Proceedings of*

IEEE ICEMS 2008 International Conference, Oct, 2008.
[18] Jung-Ik Ha, Kozo Ide, Toshihiro Sawa and Seung-Ki Sul, "Sensorless Rotor Position Estimation of an Interior Permanent-Magnet Motor from Initial states," *IEEE Trans. Industrial Applications*, vol. 39, no. 3, pp. 761-767, May/June. 2003.
[19] Ali Sarikhani and Osama A. Mohammed, "Sensorless Control of PM Synchronous Machines by Physics-Based EMF observer," *IEEE Trans. Energy Conversion*, vol. 27, no. 4, pp. 1009-1017, Dec. 2012.
[20] Start-up System for a Synchronous Motor Drive, Alberto Abbondanti, Plum Boro, Pa. (1988, May 24). 4,746,850 [U.S. Patent documents]

Hyunsung An He received the B.S. degree in physics from Chungbuk national University, Cheongju, South Korea, in 2010, the M.S. degree in electrical engineering from Chungnam National University, Daejeon, South Korea, in 2013. He is currently working toward the Ph.D. degree in electrical engineering. His research interests include static frequency converter, motor drive system, energy harvester, wave power generation system.

Hanju Cha He received the B.S. degree in electrical engineering from Seoul National University, Seoul, Korea, in 1988, the M.S. degree in electrical engineering from Pohang Institute of Science and Technology, Pohang, Korea, in 1990, and the Ph.D. degree in electrical engineering from Texas A&M University, College Station, in 2004. From 1990 to 2001, he was with LG Industrial Systems, Anyang, Korea, where he was engaged in the development of power electronics and adjustable speed drives. Since 2005, he has been with the Department of Electrical Engineering, Chungnam National University, Daejeon, Korea. He was a Visiting Professor with United Technology Research Center, Hartford, CT, USA, in 2009. His research interests are high-power converter, ac/dc, dc/ac, and ac/ac converter topologies, power quality, and utility interface issues for distributed energy system and microgrids.